



Published in final edited form as:

*Curr Opin Chem Biol.* 2021 October ; 64: 90–97. doi:10.1016/j.cbpa.2021.05.005.

## Coupling chemical biology and vibrational spectroscopy for studies of amyloids in vitro and in cells

Matthew D. Watson, Jennifer C. Lee\*

Laboratory of Protein Conformation and Dynamics, Biochemistry and Biophysics Center, National Heart, Lung, and Blood Institute, National Institutes of Health, Bethesda, Maryland, 20892, United States

### Abstract

Amyloid diseases are characterized by the aggregation of various proteins to form insoluble  $\beta$ -sheet rich fibrils leading to cell death. Vibrational spectroscopies have emerged as attractive methods to study this process due to the rich structural information that can be extracted without large, perturbative probes. Importantly, specific vibrations such as the amide-I band directly report on secondary structure changes, which are key features of amyloid formation. Beyond intrinsic vibrations, the incorporation of unnatural vibrational probes can improve sensitivity for secondary structure determination (*e.g.* isotopic labeling), provide residue-specific information of the surrounding polarity (*e.g.* unnatural amino acid), and are translatable into cellular studies. Here, we review the latest studies that have leveraged tools from chemical biology for the incorporation of novel vibrational probes into amyloidogenic proteins for both mechanistic and cellular studies.

### 1. Introduction

Amyloid diseases, including Alzheimer's (AD), Parkinson's (PD), Huntington's, and type-II diabetes are a collection of protein misfolding diseases defined by the aggregation of various proteins into amyloid fibrils [1,2]. Amyloids are unbranched, filamentous assemblies rich in  $\beta$ -sheet secondary structure. A universal characteristic is the perpendicular alignment of the individual  $\beta$ -strands with respect to the fibril axis, known as the cross- $\beta$  conformation, where the dominant interaction is hydrogen-bonding of backbone carbonyls (C=O) and amides (N-H) between monomeric units [3,4]. Additional side chain interactions such as steric zippers [5], salt bridges [6], and  $\pi$ - $\pi$  stacking [7] can contribute to stabilizing amyloid structure formation.

\*Corresponding author. leej4@nhlbi.nih.gov.

#### Declaration of interests

The authors declare that they have no known competing financial interests or personal relationships that could have appeared to influence the work reported in this paper.

**Publisher's Disclaimer:** This is a PDF file of an unedited manuscript that has been accepted for publication. As a service to our customers we are providing this early version of the manuscript. The manuscript will undergo copyediting, typesetting, and review of the resulting proof before it is published in its final form. Please note that during the production process errors may be discovered which could affect the content, and all legal disclaimers that apply to the journal pertain.

The propagation of amyloid structures through self-templating is intrinsic to their formation and has been implicated in cell-to-cell transmission in some amyloid diseases [8–10]. Amyloid formation is an inherently stochastic process, making it highly sensitive to molecular perturbations. Solution conditions (*e.g.* pH, ionic strength, and temperature), post-translational modifications (*e.g.* acetylation, phosphorylation, glycosylation), and disease-related missense mutations have been demonstrated to dramatically alter not only the rate of aggregation but also the final fibril structure [11–14].

Fibril structural complexity and polymorphism have attracted interest in the application of vibrational spectroscopies to their studies [15]. In the context of protein structure, vibrational spectroscopies are particularly sensitive to changes in the amide-I band, which is composed primarily of the backbone carbonyl (C=O) stretching mode. Backbone interactions give rise to vibrational coupling between carbonyls, leading to amide-I frequencies that are characteristic for secondary structural motifs such as  $\beta$ -sheets. Amyloid fibrils are particularly amenable to vibrational spectroscopies due to the strong coupling of the carbonyls in the cross- $\beta$  structure enhancing the intensity of the amide-I band [16–18]. Fourier-transform infrared spectroscopy (FTIR) has been extensively employed to characterize  $\beta$ -sheet structure in numerous amyloids *in vitro* [19], while Raman studies have been more limited by comparison.

Given the sensitivity of amyloid structures to solution conditions, it would be pertinent to perform secondary structural analysis in cells as it is not yet well understood how different cellular compartments and environments impact fibril structure and propagation. Case in point, recent structures of tau fibrils determined by cryoelectron microscopy of patient samples reveal that tau adopts unique structures in AD, chronic traumatic encephalopathy, Pick's disease, and corticobasal degeneration, suggesting an intimate relationship between amyloid structure and disease phenotype [20]. More recently,  $\alpha$ -synuclein ( $\alpha$ -syn) fibril structures derived from patient samples of multiple system atrophy (MSA) and PD are also distinct [21,22]. In principle, vibrational techniques are capable of detecting  $\beta$ -sheet formation even in the early stages of aggregation, and assignment to specific residues is possible [15,19]. However, there are technical challenges to overcome due to spectral interference from endogenous biomolecular vibrations and, in the case of IR, strong water absorbance near the amide-I band.

In our own work, we have used Raman spectroscopy to study fibril formation of  $\alpha$ -syn [11,23–25], which is the main amyloidogenic protein involved in PD, MSA, and dementia with Lewy bodies [26]. Notably, we have worked on the development of Raman probes towards fibril characterization in cells by Raman spectral imaging [27,28], where we have coupled a spectrometer to an inverted microscope to permit the acquisition of Raman spectra at multiple spatial locations. This is an important endeavor as there is substantial interest in observing where protein aggregation is initiated in the cell as well as to discern whether structural differences exist between aggregates in distinct cellular compartments. As part of this effort, we have utilized both isotopic labeling and unnatural amino acids (UAA) to facilitate these studies [27–29].

In this Review, we highlight work from the last three years leveraging chemical biological approaches such as expressed-protein ligation, metabolic labeling, and biosynthetic incorporation to install different vibrational probes in amyloidogenic proteins *in vitro* and in cells. Two major classes of vibrational probes are discussed— isotopic labeling and UAA incorporation. Isotopic labels offer the advantage of minimal perturbation and can enable site-specific examination of secondary structure, while UAAs can be used to introduce a wide variety of chemically and spectrally unique groups. The application of chemical biology to incorporate vibrational probes has significant potential to enable spectroscopic interrogations of protein misfolding and aggregation in cellular systems, which will contribute towards the mechanistic understanding of amyloid fibrils and their behaviors in diseases.

## 2. Isotopic Labeling

One approach to extracting residue-specific information is the use of isotopic labeling to shift vibrational modes of interest into a unique spectral region. Replacement of any nuclei involved in a vibrational mode, such as  $^{13}\text{C}$ -labeling of a backbone carbonyl shifts that vibrational mode to lower wavenumbers due to the change in reduced mass. Isotopic labeling has long been an attractive strategy in large part due to the minimally perturbative nature of these modifications. In its simplest form, isotopic labeling can be easily accomplished by expressing the protein of interest in isotope-enriched media or through use of isotopically-labeled amino acids in solid-phase peptide synthesis (SPPS). Okada *et al.* recently exemplified this approach in a study of amyloid- $\beta$  ( $\text{A}\beta$ ), which is the amyloidogenic protein involved in AD [30]. The authors incorporated  $^{13}\text{C}$ -carbonyls at specific sites using SPPS and measured carbonyl coupling in the  $\beta$ -sheet structure of these aggregates by FTIR. Using curve-fitting analysis, it was concluded that  $\text{A}\beta$  aggregates on GM1 lipid clusters are composed of unusual mixed parallel/antiparallel  $\beta$ -sheets, which are not observed for  $\text{A}\beta$  fibrils formed in solution.

Spectral resolution can be further enhanced by double isotopic labeling, such as by  $^{13}\text{C}^{18}\text{O}$ -carbonyl labeling as demonstrated in prior work [31–33]. Zanni and coworkers have made extensive use of  $^{13}\text{C}^{18}\text{O}$ -labeling in their two-dimensional IR (2D-IR) experiments with human islet amyloid polypeptide (hIAPP), which forms extracellular amyloid plaques in type-II diabetes [34,35]. For a full discussion on 2D-IR, we refer the reader to the many reviews on the topic [36–39]. Briefly, separate pump and probe lasers are used to produce a correlation map of vibrational coupling between functional groups. Interactions between residues appear as off-diagonal peaks in a manner analogous to two-dimensional NMR experiments, though 2D-IR is sensitive to events on much faster timescales. In addition to enhanced structural information, this method also offers significant improvements in sensitivity. 2D-IR has been used to identify amyloid in human cataracts and a novel hIAPP polymorph in human serum as well as in the design of a biosensor of protein structure [40–42]. More recently, Maj *et al.* demonstrated 2D-IR methods to study interactions between specific residue pairs by double-labeling hIAPP with  $^{13}\text{C}^{18}\text{O}$ , revealing the existence of transient helical structure preceding oligomer formation [43]. Isotopic labeling can also be employed to probe side chain interactions, such as DeGrado and coworkers' recent

demonstration of Gln ladder formation in Tau<sub>306–311</sub> and a yeast prion-derived peptide using a  $^{13}\text{C}^{18}\text{O}$ -labeled Gln sidechain [44].

### 2.1. Raman study of segmentally $^{13}\text{C}$ -labeled $\alpha$ -synuclein

Through the use of segmental  $^{13}\text{C}$ -labeling, we extended this approach to the study of specific polypeptide regions in  $\alpha$ -syn [29]. Intein-mediated ligation was used to prepare  $\alpha$ -syn uniformly labeled with  $^{13}\text{C}$  in the first 86 residues and  $^{12}\text{C}$  in the remaining 54 C-terminal residues (Fig. 1A). To accomplish this,  $\alpha$ -syn was expressed in two segments in *E. coli*. This approach is analogous to a previous 2D-IR study by Moran *et al.* on the aggregation mechanism of segmentally  $^{13}\text{C}$ -labeled  $\gamma\text{D}$ -crystallin [45]. Briefly, residues 1–86 were expressed with a C-terminal intein-tag followed by a chitin binding domain in  $^{13}\text{C}$ -enriched media, while residues 87–140 with a Ser-to-Cys mutation at position 87 were expressed in natural isotope abundance media. Autocleavage of the intein in the presence of a thiol produces an C-terminal thioester that reacts with the mutant Cys residue to generate the ligated S87C- $\alpha$ -syn with residues 1–86 and 87–140 uniformly labeled with  $^{13}\text{C}$  and  $^{12}\text{C}$ , respectively. This ligation reaction was performed as a one-pot synthesis, where the C-terminal fragment was supplemented in the cleavage buffer as the protein is released from the chitin column. Due to the intrinsically disordered nature of  $\alpha$ -syn, the coupling was facile.

The ligated protein produces two discrete amide-I bands in the Raman spectrum, permitting simultaneous secondary structural analysis of both regions (Fig. 1B). Raman spectral imaging enabled examination of early aggregates, which revealed the existence of a kinetic intermediate that displays a sharp  $^{13}\text{C}$ -amide-I peak, but a broad  $^{12}\text{C}$ -amide-I band. This suggests that early aggregation of  $\alpha$ -syn involves the formation of  $\beta$ -sheet structure in the N-terminal region that later propagates into the C-terminal region of the protein. This work underscores the strength of coupling the chemical biological approach of chemical ligation with vibrational spectroscopy which provides unique information on secondary structure.

### 2.2. Raman spectral imaging of $^{13}\text{C}^2\text{H}^{15}\text{N}$ -labeled $\alpha$ -synuclein fibrils in cells

Recently, we reported a different approach using uniformly  $^{13}\text{C}^2\text{H}^{15}\text{N}$ -labeled  $\alpha$ -syn. The advantage here is the capability of resolving  $\alpha$ -syn from endogenous proteins in a cellular environment due to the presence of the  $^{13}\text{C}$ - $^2\text{H}$  stretching bands, which appear in the center of the cellular quiet spectral region (Fig. 2A). The cellular quiet region is a region of the vibrational spectrum from  $\sim 1800$  to  $2400\text{ cm}^{-1}$  where no naturally-occurring biomolecules are vibrationally active.

This isotopically labeled protein was used to examine fibril endocytosis, which is thought to be a key component of disease progression in synucleinopathies [46]. In this process, healthy cells uptake fibrils which seed amyloid formation of the endogenous soluble  $\alpha$ -syn, leading to fibril propagation and cytotoxicity. Preformed  $^{13}\text{C}^2\text{H}^{15}\text{N}$ -labeled fibrils were fed to cultured mammalian cells and mapped by Raman spectral imaging to examine the fate of these endocytosed fibrils (Fig. 2B) [28]. Our data demonstrate that the  $^{13}\text{C}^2\text{H}^{15}\text{N}$ -amide-I band can be resolved from other cellular vibrational signals and that the strong  $^{13}\text{C}$ - $^2\text{H}$  stretching bands enable background-free mapping of exogenous  $\alpha$ -syn in cells (Fig. 2C).

Comparison of the amide-I band to the  $^{13}\text{C}$ - $^2\text{H}$  stretching modes, which are relatively insensitive to structural changes indicate that there is no appreciable loss of  $\beta$ -sheet structure upon endocytosis within our experimental timeframe of 24 h. In addition, we observed that the internalized fibrils largely accumulate at the cellular periphery, colocalizing with proteins and lipids. Interestingly, we observed lipid accumulation throughout the cytoplasm. This work demonstrates unambiguous localization of internalized fibrils and direct observation of  $\beta$ -sheet structure of amyloid fibrils in cells.

### 2.3. Stimulated-Raman imaging and selective deuteration of Gln residues of polyQ aggregates in cells

Isotopic labeling has recently been demonstrated for imaging aggregates formed from endogenous proteins. PolyQ diseases, including Huntington's disease are characterized by translation of long chains of glutamine residues at the C-terminus of proteins such as Huntingtin [47]. These polyQ repeats trigger intracellular amyloid formation and subsequent cell death. Miao and Wei took advantage of the enrichment of Gln in these aggregates by introducing deuterium labeled Gln into the growth media of cells expressing these proteins [48]. Cells were imaged using stimulated Raman scattering (SRS), a two-photon approach which offers significantly enhanced intensity for a targeted vibrational mode compared to spontaneous Raman events [49]. Notably, it was suggested that comparable contrast is achieved to that of GFP fluorescence or fluorophore staining. Since Raman imaging is quantitative, it is superior to fluorescence methods, which can be complicated in very high density aggregates due to self-quenching or impermeability to exogenous fluorophores. The structure of intracellular aggregates was further interrogated by SRS analysis of the amide-I band. Interestingly, a blue-shift associated with  $\beta$ -sheet enrichment was not detectable, in agreement with other recent work [50]. Although this approach is not widely applicable as most amyloids are not so highly enriched in a single amino acid, the sensitivity of this technique stands out from other vibrational imaging methods in cells.

## 3. Unnatural Amino Acids

Although isotopic labeling offers the advantage of being inherently nonperturbative, the choice of labels and methods for site-specific incorporation are quite limited, especially *in vivo*. An alternative approach is UAA incorporation, which can be used to introduce a wide variety of chemically and spectroscopically unique functionalities into proteins. UAAs have been incorporated into a variety of peptides and proteins both by SPPS and chemical biology methods. UAAs such as 4-cyano-L-phenylalanine and azidohomoalanine are well studied and successful vibrational probes of protein folding [51–53]. In the context of amyloids, the use of UAAs as infrared probes has been largely limited to synthetic peptides [54–56]. One recent study, Pazos *et al.* employed two UAAs to examine  $\text{A}\beta_{16-22}$  hydrogen-bonding dynamics [57]. They introduced an ester group *via* an Asp derivative, L-aspartic acid 4-methyl ester ( $\text{D}_\text{M}$ ) and a second UAA, Lys(Nvoc) to improve fibril homogeneity. The authors used the unique vibrational band of  $\text{D}_\text{M}$  to demonstrate that this position is exposed to two distinct chemical environments, one which is buried and the other solvent-exposed. Using the structural constraints from the FTIR data, a structural model of two antiparallel  $\beta$ -sheets packed parallel to one another was proposed. In a demonstration of the exquisite

time resolution of vibrational spectroscopies, the authors also examined 2D-IR picosecond spectral diffusion dynamics to detect the  $D_M$  carbonyl switching between H-bonds with individual hydrogens on a Lys amino-group.

### 3.1. Homopropargylglycine, a terminal alkyne Raman probe for cellular studies

In cells, the most straightforward method of unnatural amino acid incorporation is biosynthetic incorporation, which we employed in our own work with the alkyne-containing amino acid homopropargylglycine (HPG). HPG is a methionine analogue and was first introduced into proteins by Tirrell and coworkers, although they used it for bioorthogonal fluorophore labeling [58–60]. Others have used it as a metabolic label of the proteome in stimulated Raman imaging [61]. Here, HPG was introduced into  $\alpha$ -syn biosynthetically in *E. coli* [27]. Because cells cannot distinguish HPG from methionine, Met residues can be readily replaced with HPG in a Met-auxotrophic strain of *E. coli* (Fig. 3A). The stretching vibrational mode of the alkynyl functional group appears at  $\sim 2110\text{ cm}^{-1}$  in the middle of the cellular quiet region (Fig. 3B). The alkyne moiety is sensitive to the polarity of its local surroundings, shifting to lower energies in more hydrophobic environments.

Since  $\alpha$ -syn contains four native Met residues at positions 1, 5, 116 and 127, the alkyne stretching band of HPG-labeled  $\alpha$ -syn simultaneously reports on the local environments of the N- and C-termini. To examine these ends independently, a C-terminally truncated variant comprising residues 1–115 was also studied. Whereas the alkyne stretching bands of HPG- $\alpha$ -syn and HPG- $\alpha$ -syn<sub>1–115</sub> fibrils were similar *in vitro*, the peak narrowed and blue-shifted for HPG- $\alpha$ -syn<sub>1–115</sub> when measured in cultured N27 rat dopaminergic cells (Fig. 3C). This suggests that the N- and C-termini experience very different local environments in cells, despite recent cryo-EM structures indicating that neither region is well-structured in the fibrillar state (Fig. 3A) [24,62,63].

By coupling HPG- and  $^{13}\text{C}$ -labeling of  $\alpha$ -syn, it was also possible to analyze protein secondary structure in the cellular environment, which suggested that although removal of the C-terminus did not significantly affect  $\beta$ -sheet formation, it did lead to reduced lipid accumulation. To our knowledge, this is the first Raman study of protein-lipid interactions and amyloid formation using HPG. Furthermore, it is also the first reported direct observation of  $\beta$ -sheet secondary structure and region-specific differences in  $\alpha$ -syn fibrils in cellular environments.

## 4. Conclusions and Outlook

The vibrational spectroscopic studies reviewed here exemplify the utility and versatility of the probes and methods available to study amyloids from the atomic to cellular scale. Vibrational probes can be very small and minimally perturbative, making them particularly attractive in amyloid formation studies. Though a variety of vibrational probes have been incorporated into amyloidogenic proteins by SPPS, the work reviewed here demonstrates the efforts to extend this approach to a wider array of amyloids. Despite their potential, vibrational studies in cells are underexplored, highlighting a tremendous opportunity for further advances in this area. As amyloid research moves towards understanding fibril formation by larger, more complex proteins and in cellular environments, new methods



of vibrational probe incorporation are needed. Perhaps the most notable absence among these methods is UAA incorporation using evolved aminoacyl-tRNA/tRNA pairs (21<sup>st</sup>-pair technology). This approach has been employed to incorporate a variety of vibrational probes for protein folding studies, but remains an untapped resource in amyloid research. It has been demonstrated in prokaryotic and eukaryotic expression systems, as well as cultured mammalian cells, making it an attractive and vetted method for both *in vitro* and *in cellulo* studies [64]. As this field continues to develop, we expect that chemical biology will play an increasingly prominent role in vibrational spectroscopic studies of amyloid formation.

## Acknowledgements.

MDW and JCL are supported by the Intramural Research Program at the National Institutes of Health, National Heart, Lung, and Blood Institute.

## Abbreviations

<b>AD</b>	Alzheimer's disease
<b>PD</b>	Parkinson's disease
<b>FTIR</b>	Fourier-transform infrared spectroscopy
<b><math>\alpha</math>-syn</b>	$\alpha$ -synuclein
<b>MSA</b>	multiple system atrophy
<b>UAA</b>	unnatural amino acid
<b>SPPS</b>	solid-phase peptide synthesis
<b>A<math>\beta</math></b>	amyloid- $\beta$
<b>2D-IR</b>	two-dimensional infrared spectroscopy
<b>hIAPP</b>	human islet amyloid polypeptide
<b>MESNA</b>	2-mercaptoethanesulfonate
<b>SRS</b>	stimulated Raman scattering
<b>D<sub>M</sub></b>	L-aspartic acid 4-methyl ester
<b>HPG</b>	homopropargylglycine

## Annotated References

Papers of particular interest, published within the period of review, have been highlighted as:

- of special interest
- of outstanding interest

1. Chiti F, Dobson CM: Protein misfolding, functional amyloid, and human disease. *Ann Rev Biochem* 2006, 75:333–366.

2. Selkoe DJ: Folding proteins in fatal ways. *Nature* 2003, 426:900–904. [PubMed: 14685251]
3. Eisenberg DS, Sawaya MR: Structural studies of amyloid proteins at the molecular level. *Ann Rev Biochem* 2017, 86:69–95.
4. Jahn TR, Makin OS, Morris KL, Marshall KE, Tian P, Sikorski P, Serpell LC: The common architecture of cross- $\beta$  amyloid. *J Mol Biol* 2010, 395:717–727. [PubMed: 19781557]
5. Sawaya MR, Sambashivan S, Nelson R, Ivanova MI, Sievers SA, Apostol MI, Thompson MJ, Balbirnie M, Wiltzius JJ, McFarlane HT, et al. : Atomic structures of amyloid cross- $\beta$  spines reveal varied steric zippers. *Nature* 2007, 447:453–457. [PubMed: 17468747]
6. Boyer DR, Li B, Sun C, Fan W, Zhou K, Hughes MP, Sawaya MR, Jiang L, Eisenberg DS: The  $\alpha$ -synuclein hereditary mutation E46K unlocks a more stable, pathogenic fibril structure. *Proc Natl Acad Sci USA* 2020, 117:3592–3602. [PubMed: 32015135]
7. Makin OS, Atkins E, Sikorski P, Johansson J, Serpell LC: Molecular basis for amyloid fibril formation and stability. *Proc Natl Acad Sci USA* 2005, 102:315–320. [PubMed: 15630094]
8. Harper JD, Lansbury PT Jr.: Models of amyloid seeding in Alzheimer’s disease and scrapie: Mechanistic truths and physiological consequences of the time-dependent solubility of amyloid proteins. *Ann Rev Biochem* 1997, 66:385–407.
9. Powers ET, Powers DL: Mechanisms of protein fibril formation: nucleated polymerization with competing off-pathway aggregation. *Biophys J* 2008, 94:379–391. [PubMed: 17890392]
10. Guo JL, Lee VM: Cell-to-cell transmission of pathogenic proteins in neurodegenerative diseases. *Nat Med* 2014, 20:130–138. [PubMed: 24504409]
11. Watson MD, Lee JC: N-terminal acetylation affects  $\alpha$ -synuclein fibril polymorphism. *Biochemistry* 2019, 58:3630–3633. [PubMed: 31424918]
12. Sneideris T, Darguzis D, Botyriute A, Grigaliunas M, Winter R, Smirnovas V: pH-driven polymorphism of insulin amyloid-like fibrils. *PLoS One* 2015, 10:e0136602. [PubMed: 26313643]
13. Guerrero-Ferreira R, Kovacic L, Ni D, Stahlberg H: New insights on the structure of  $\alpha$ -synuclein fibrils using cryo-electron microscopy. *Curr Opin Neurobiol* 2020, 61:89–95.
14. Li D, Liu C: Hierarchical chemical determination of amyloid polymorphs in neurodegenerative disease. *Nat Chem Biol* 2021, 10.1038/s41589-020-00708-z.
15. Li H, Lantz R, Du D: Vibrational approach to the dynamics and structure of protein amyloids. *Molecules* 2019, 24.
16. Sarroukh R, Goormaghtigh E, Ruyschaert JM, Raussens V: ATR-FTIR: a “rejuvenated” tool to investigate amyloid proteins. *Biochim Biophys Acta* 2013, 1828:2328–2338. [PubMed: 23746423]
17. Lomont JP, Ostrander JS, Ho JJ, Petti MK, Zanni MT: Not all  $\beta$ -sheets are the same: Amyloid infrared spectra, transition dipole strengths, and couplings investigated by 2D IR spectroscopy. *J Phys Chem B* 2017, 121:8935–8945. [PubMed: 28851219]
18. Zandomenighi G, Krebs MR, McCammon MG, Fandrich M: FTIR reveals structural differences between native  $\beta$ -sheet proteins and amyloid fibrils. *Protein Sci* 2004, 13:3314–3321. [PubMed: 15537750]
19. Moran SD, Zanni MT: How to get insight into amyloid structure and formation from infrared spectroscopy. *J Phys Chem Lett* 2014, 5:1984–1993. [PubMed: 24932380]
20. Scheres SH, Zhang W, Falcon B, Goedert M: Cryo-EM structures of tau filaments. *Curr Opin Struct Biol* 2020, 64:17–25. [PubMed: 32603876]
21. Schweighauser M, Shi Y, Tarutani A, Kametani F, Murzin AG, Ghetti B, Matsubara T, Tomita T, Ando T, Hasegawa K, et al. : Structures of  $\alpha$ -synuclein filaments from multiple system atrophy. *Nature* 2020, 585:464–469. [PubMed: 32461689]
22. Shah Nawaz M, Mukherjee A, Pritzkow S, Mendez N, Rabadia P, Liu X, Hu B, Schmeichel A, Singer W, Wu G, et al. : Discriminating  $\alpha$ -synuclein strains in Parkinson’s disease and multiple system atrophy. *Nature* 2020, 578:273–277. [PubMed: 32025029]
23. Flynn JD, McGlinchey RP, Walker RL 3rd, Lee JC: Structural features of  $\alpha$ -synuclein amyloid fibrils revealed by Raman spectroscopy. *J Biol Chem* 2018, 293:767–776. [PubMed: 29191831]
24. Ni X, McGlinchey RP, Jiang J, Lee JC: Structural insights into  $\alpha$ -synuclein fibril polymorphism: effects of Parkinson’s disease-related C-terminal truncations. *J Mol Biol* 2019, 431:3913–3919. [PubMed: 31295458]



25. Flynn JD, Lee JC: Raman fingerprints of amyloid structures. *Chem Commun (Camb)* 2018, 54:6983–6986. [PubMed: 29774336]
26. Lees AJ, Hardy J, Revesz T: Parkinson's disease. *Lancet* 2009, 373:2055–2066. [PubMed: 19524782]
- 27. Flynn JD, Gimmen MY, Dean DN, Lacy SM, Lee JC: Terminal alkynes as Raman probes of  $\alpha$ -synuclein in solution and in cells. *ChemBioChem* 2020, 21:1582–1586. [PubMed: 31960993] Using a Met-auxotrophic expression system, the unnatural amino acid HPG was biosynthetically incorporated into  $\alpha$ -syn. Analysis of the alkyne stretching band by Raman spectral imaging revealed local sidechain differences in the cellularly internalized fibrils.
- 28. Watson MD, Flynn JD, Lee JC: Raman spectral imaging of  $(^{13}\text{C}(2)\text{H}(15)\text{N})$ -labeled  $\alpha$ -synuclein amyloid fibrils in cells. *Biophys Chem* 2021, 269:106528. [PubMed: 33418468] Raman spectral imaging of cells treated with  $^{13}\text{C}^2\text{H}^{15}\text{N}$ -labeled  $\alpha$ -syn fibrils demonstrated background-free detection and colocalization of  $\beta$ -sheet amyloid structure with endogenous biomolecules in a cellular environment.
- 29. Flynn JD, Jiang Z, Lee JC: Segmental  $^{13}\text{C}$ -labeling and Raman microspectroscopy of  $\alpha$ -synuclein amyloid formation. *Atigew Chem Int Ed Engl* 2018, 57:17069–17072. A method for segmental  $^{13}\text{C}$ -labeling of  $\alpha$ -syn using intein-mediated expressed-protein ligation was reported. Aggregation kinetics were monitored by the respective amide-I bands revealing region-specific  $\beta$ -sheet structural changes.
- 30. Okada Y, Okubo K, Ikeda K, Yano Y, Hoshino M, Hayashi Y, Kiso Y, Itoh-Watanabe H, Naito A, Matsuzaki K: Toxic amyloid tape: A novel mixed antiparallel/parallel  $\beta$ -sheet structure formed by amyloid  $\beta$ -protein on GM1 clusters. *ACS Chem Neurosci* 2019, 10:563–572. The authors measured carbonyl coupling in  $^{13}\text{C}$ -labeled A $\beta$  fibrils to demonstrate the formation of unusual mixed parallel/antiparallel  $\beta$ -sheet structures on GM1 lipid clusters.
31. Brewer SH, Song B, Raleigh DP, Dyer RB: Residue specific resolution of protein folding dynamics using isotope-edited infrared temperature jump spectroscopy. *Biochemistry* 2007, 46:3279–3285. [PubMed: 17305369]
32. Davis CM, Cooper AK, Dyer RB: Fast helix formation in the B domain of protein A revealed by site-specific infrared probes. *Biochemistry* 2015, 54:1758–1766. [PubMed: 25706439]
33. Fang C, Wang J, Charnley AK, Barber-Armstrong W, Smith Iii AB, Decatur SM, Hochstrasser RM: Two-dimensional infrared measurements of the coupling between amide modes of an  $\alpha$ -helix. *Chem Phys Lett* 2003, 382:586–592.
34. Buchanan LE, Maj M, Dunkelberger EB, Cheng PN, Nowick JS, Zanni MT: Structural polymorphs suggest competing pathways for the formation of amyloid fibrils that diverge from a common intermediate species. *Biochemistry* 2018, 57:6470–6478. [PubMed: 30375231]
35. Serrano AL, Lomont JP, Tu LH, Raleigh DP, Zanni MT: A free energy barrier caused by the refolding of an oligomeric intermediate controls the lag time of amyloid formation by hIAPP. *J Am Chem Soc* 2017, 139:16748–16758. [PubMed: 29072444]
36. Ganim Z, Chung HS, Smith AW, Deflores LP, Jones KC, Tokmakoff A: Amide I two-dimensional infrared spectroscopy of proteins. *Acc Chem Res* 2008, 41:432–441. [PubMed: 18288813]
37. Ghosh A, Ostrander JS, Zanni MT: Watching proteins wiggle: Mapping structures with two-dimensional infrared spectroscopy. *Chem Rev* 2017, 117:10726–10759. [PubMed: 28060489]
38. Kraack JP, Hamm P: Surface-sensitive and surface-specific ultrafast two-dimensional vibrational spectroscopy. *Chem Rev* 2017, 117:10623–10664. [PubMed: 28830147]
39. Le Sueur AL, Horness RE, Thielges MC: Applications of two-dimensional infrared spectroscopy. *Analyst* 2015, 140:4336–4349. [PubMed: 26007625]
40. Alperstein AM, Ostrander JS, Zhang TO, Zanni MT: Amyloid found in human cataracts with two-dimensional infrared spectroscopy. *Proc Natl Acad Sci USA* 2019, 116:6602–6607. [PubMed: 30894486]
41. Fields CR, Dicke SS, Petti MK, Zanni MT, Lomont JP: A different hIAPP polymorph is observed in human serum than in aqueous buffer: demonstration of a new method for studying amyloid fibril structure using infrared spectroscopy. *J Phys Chem Lett* 2020, 11:6382–6388. [PubMed: 32706257]

42. Ostrandner JS, Lomont JP, Rich KL, Saraswat V, Feingold BR, Petti MK, Birdsall ER, Arnold MS, Zanni MT: Monolayer sensitivity enables a 2D IR spectroscopic immuno-biosensor for studying protein structures: Application to amyloid polymorphs. *J Phys Chem Lett* 2019, 10:3836–3842. [PubMed: 31246039]
- 43. Maj M, Lomont JP, Rich KL, Alperstein AM, Zanni MT: Site-specific detection of protein secondary structure using 2D IR dihedral indexing: A proposed assembly mechanism of oligomeric hIAPP. *Chem Sci* 2018, 9:463–474. [PubMed: 29619202] Vibrational coupling between pairs of  $^{13}\text{C}^{18}\text{O}$ -labeled residues in hIAPP was measured by 2D-IR and used to identify transient helical structure in a prefibrillar species.
- 44. Wu H, Saltzberg DJ, Kratochvil HT, Jo H, Sali A, DeGrado WF: Glutamine side chain  $^{13}\text{C}$ - $^{18}\text{O}$  as a nonperturbative IR probe of amyloid fibril hydration and assembly. *J Am Chem Soc* 2019, 141:7320–7326. [PubMed: 30998340] FTIR-based isotope dilution experiments using  $^{13}\text{C}^{18}\text{O}$ -labeled Gln sidechains in peptides revealed the formation of Gln ladders in yeast prion and tau-derived peptides.
45. Moran SD, Woys AM, Buchanan LE, Bixby E, Decatur SM, Zanni MT: Two-dimensional IR spectroscopy and segmental  $^{13}\text{C}$  labeling reveals the domain structure of human  $\gamma\text{D}$ -crystallin amyloid fibrils. *Proc Natl Acad Sci USA* 2012, 109:3329–3334. [PubMed: 22328156]
46. Rodriguez L, Marano MM, Tandon A: Import and export of misfolded  $\alpha$ -synuclein. *Front Neurosci* 2018, 12:344.
47. Fan HC, Ho LI, Chi CS, Chen SJ, Peng GS, Chan TM, Lin SZ, Harn HJ: Polyglutamine (PolyQ) diseases: Genetics to treatments. *Cell Transplant* 2014, 23:441–458. [PubMed: 24816443]
- 48. Miao K, Wei L: Live-cell imaging and quantification of polyQ aggregates by stimulated Raman scattering of selective deuterium labeling. *ACS Cent Sci* 2020, 6:478–486. [PubMed: 32341997] Quantitative imaging of endogenous poly-Q aggregates in live cells was accomplished using stimulated Raman scattering by introduction of deuterated Gln into growth media.
49. Freudiger CW, Min W, Saar BG, Lu S, Holtom GR, He C, Tsai JC, Kang JX, Xie XS: Label-free biomedical imaging with high sensitivity by stimulated Raman scattering microscopy. *Science* 2008, 322:1857–1861. [PubMed: 19095943]
50. Warner JBt, Ruff KM, Tan PS, Lemke EA, Pappu RV, Lashuel HA: Monomeric huntingtin exon 1 has similar overall structural features for wild-type and pathological polyglutamine lengths. *J Am Chem Soc* 2017, 139:14456–14469. [PubMed: 28937758]
51. Bagchi S, Boxer SG, Fayer MD: **Ribonuclease S dynamics measured using a nitrile label with 2D IR vibrational echo spectroscopy.** *J Phys Chem B* 2012, 116:4034–4042. [PubMed: 22417088]
52. Chung JK, Thielges MC, Fayer MD: **Conformational dynamics and stability of HP35 studied with 2D IR vibrational echoes.** *J Am Chem Soc* 2012, 134:12118–12124. [PubMed: 22764745]
53. Taskent-Sezgin H, Chung J, Banerjee PS, Nagarajan S, Dyer RB, Carrico I, Raleigh DP: Azidohomoalanine: A conformationally sensitive IR probe of protein folding, protein structure, and electrostatics. *Angew Chem Int Ed Engl* 2010, 49:7473–7475. [PubMed: 20815000]
54. Jia B, Sun Y, Yang L, Yu Y, Fan H, Ma G: A structural model of the hierarchical assembly of an amyloid nanosheet by an infrared probe technique. *Phys Chem Chem Phys* 2018, 20:27261–27271. [PubMed: 30187048]
55. Marek P, Mukherjee S, Zanni MT, Raleigh DP: **Residue-specific, real-time** characterization of lag-phase species and fibril growth during amyloid formation: A combined fluorescence and IR study of p-cyanophenylalanine analogs of islet amyloid polypeptide. *J Mol Biol* 2010, 400:878–888. [PubMed: 20630475]
56. Oh KI, Lee JH, Joo C, Han H, Cho M:  $\beta$ -Azidoalanine as an IR probe: Application to amyloid A $\beta$ (16–22) aggregation. *J Phys Chem B* 2008, 112:10352–10357. [PubMed: 18671422]
- 57. Pazos IM, Ma J, Mukherjee D, Gai F: **Ultrafast hydrogen-bonding dynamics in amyloid** fibrils. *J Phys Chem B* 2018, 122:11023–11029. [PubMed: 29883122] The ester moiety of a methylated Asp residue was used as a vibrational probe of intersheet hydrogen bonding in fibrils formed by an A $\beta$ -derived peptide.
58. van Hest JCM, Kiick KL, Tirrell DA: Efficient incorporation of unsaturated methionine analogues into proteins in vivo. *J Am Chem Soc* 2000, 122:1282–1288.

59. Beatty KE, Tirrell DA: Two-color labeling of temporally defined protein populations in mammalian cells. *Bioorg Med Chem Lett* 2008, 18:5995–5999. [PubMed: 18774715]
60. Beatty KE, Xie F, Wang Q, Tirrell DA: Selective dye-labeling of newly synthesized proteins in bacterial cells. *J Am Chem Soc* 2005, 127:14150–14151. [PubMed: 16218586]
61. Wei L, Hu F, Shen Y, Chen Z, Yu Y, Lin CC, Wang MC, Min W: Live-cell imaging of alkyne-tagged small biomolecules by stimulated Raman scattering. *Nat Methods* 2014, 11:410–412. [PubMed: 24584195]
62. Guerrero-Ferreira R, Taylor NM, Mona D, Ringler P, Lauer ME, Riek R, Britschgi M, Stahlberg H: Cryo-EM structure of  $\alpha$ -synuclein fibrils. *Elife* 2018, 7:e36402. [PubMed: 29969391]
63. Li B, Ge P, Murray KA, Sheth P, Zhang M, Nair G, Sawaya MR, Shin WS, Boyer DR, Ye S, et al. : Cryo-EM of full-length  $\alpha$ -synuclein reveals fibril polymorphs with a common structural kernel. *Nat Comm* 2018, 9:3609.
64. Young DD, Schultz PG: Playing with the molecules of life. *ACS Chem Biol* 2018, 13:854–870. [PubMed: 29345901]

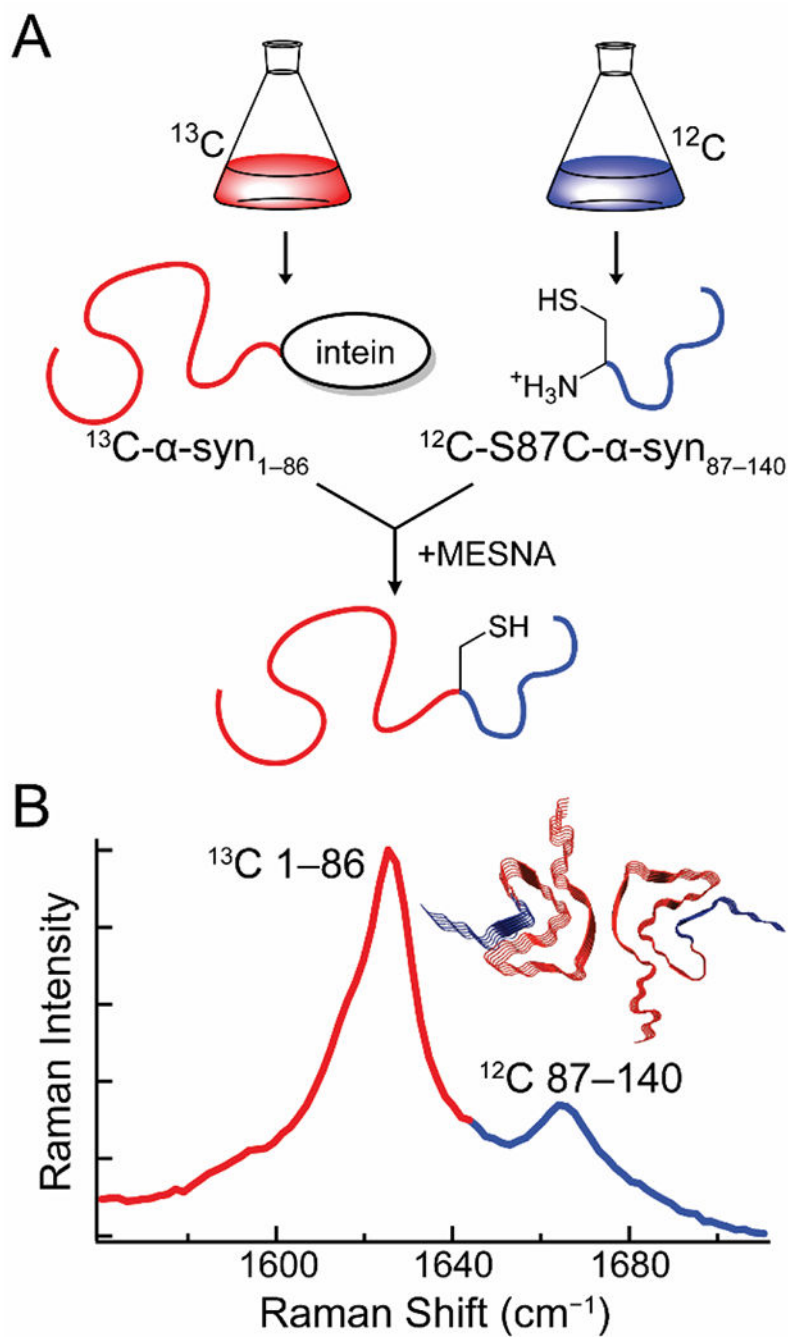


**Figure 1.** Expressed-protein ligation enables the creation of S87C- $\alpha$ -syn segmentally labeled with  $^{13}\text{C}$  and  $^{12}\text{C}$  at residues 1–86 and 87–140, respectively. (A)  $\alpha$ -Syn $_{1-86}$  is expressed with a C-terminal intein-tag in  $^{13}\text{C}$ -media, while S87C- $\alpha$ -syn is expressed in natural isotope abundance media. A one-pot reaction is carried out where autocleavage of the intein-tag in the presence of 2-mercaptoethanesulfonate (MESNA) leads to covalent ligation of the N- and C-terminal segments of the protein. (B) The  $^{13}\text{C}$ - and  $^{12}\text{C}$ -labeled segments of the fibrils produce two amide-I bands, enabling independent analysis of their secondary structures.

(Inset) Fibril structure of  $\alpha$ -syn with the  $^{13}\text{C}$ - and  $^{12}\text{C}$ -labeled fragments colored red and blue, respectively. Data originally published in [29].

Author Manuscript

Author Manuscript

Author Manuscript

Author Manuscript

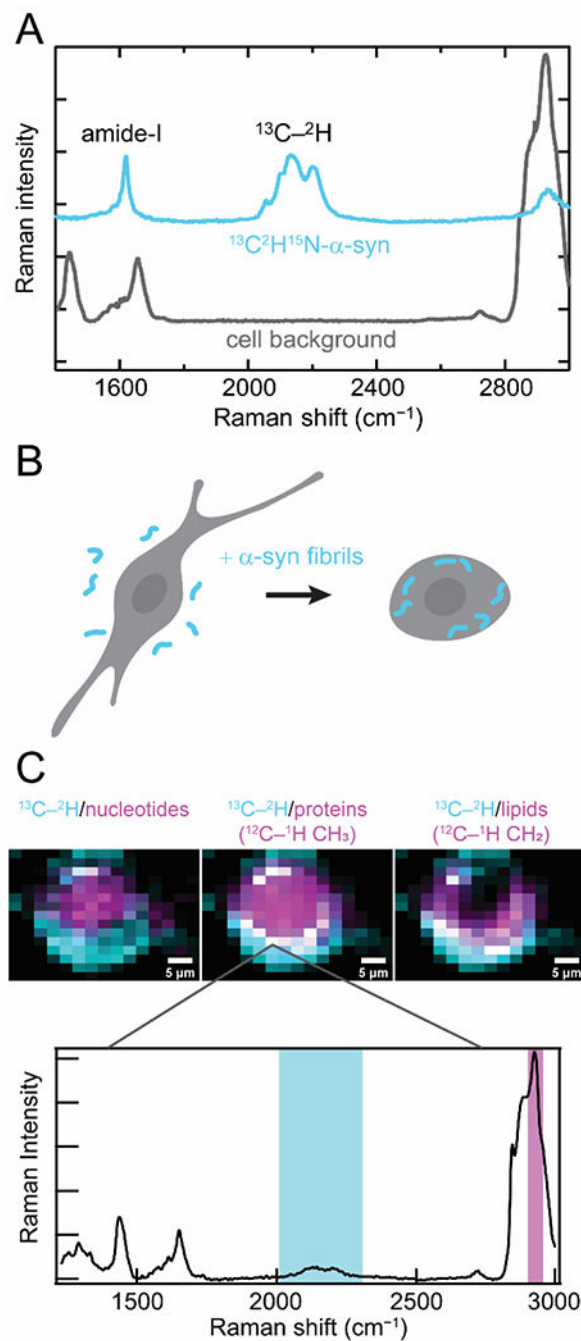


**Figure 2.** Raman spectral imaging of internalized <sup>13</sup>C<sup>2</sup>H<sup>15</sup>N- $\alpha$ -syn fibrils in cells. (A) <sup>13</sup>C<sup>2</sup>H<sup>15</sup>N- $\alpha$ -syn (cyan) possesses several unique Raman features that distinguish it against a cellular background (gray). The amide-I band is shifted to lower energy relative to endogenous amide-I and lipid C=C stretching bands, and the <sup>13</sup>C-<sup>2</sup>H stretching bands appear in the cellular quiet region. (B) Schematic representation of our experimental conditions where <sup>13</sup>C<sup>2</sup>H<sup>15</sup>N- $\alpha$ -syn fibrils formed *in vitro* (cyan) are added in media and readily taken up by cultured mammalian cells. (C) Raman maps of internalized fibrils (cyan) and



comparison to the localization of cellular components (magenta) by integrating over spectral regions characteristic of nucleotides, proteins, and lipids in human SK-MEL-28 cells (Top). Colocalization appears as white pixels. (Bottom) An example Raman spectrum measured at a pixel where  $\alpha$ -syn fibrils are colocalized with endogenous proteins. Integrated spectral regions are indicated. Data originally published in [28].

Author Manuscript

Author Manuscript

Author Manuscript

Author Manuscript

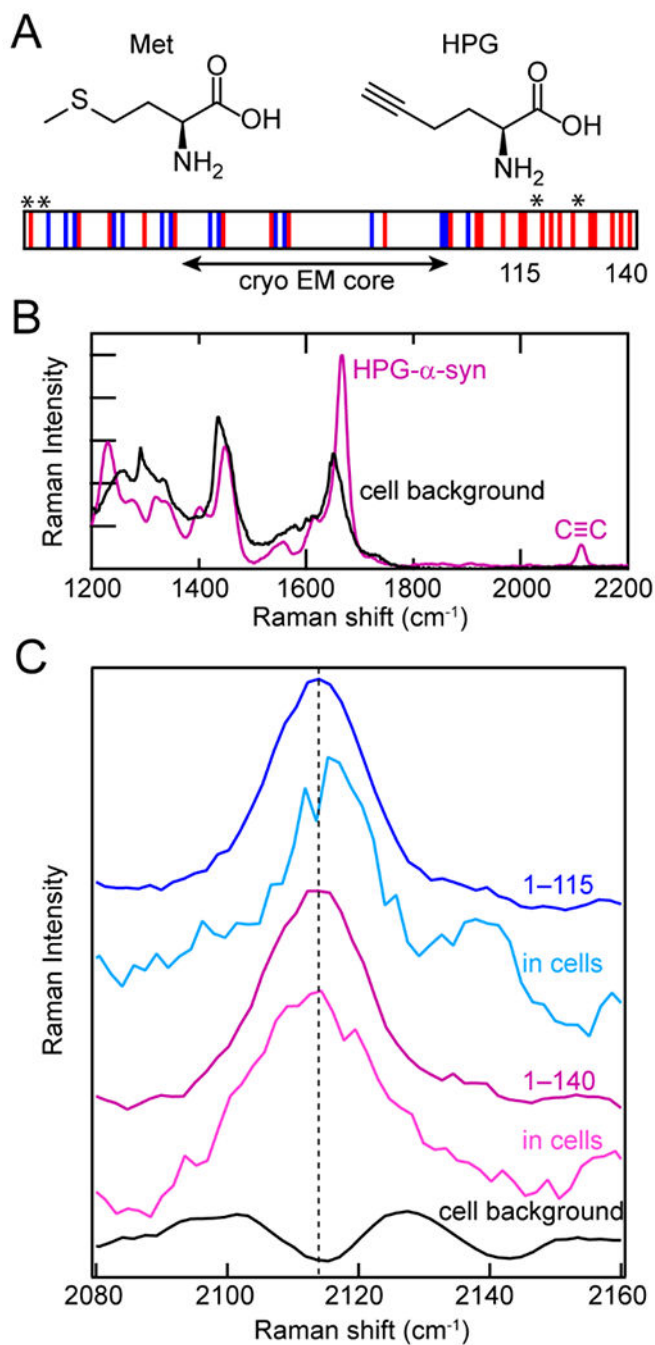


**Figure 3.** Biosynthetic incorporation of HPG, a Met analogue, into  $\alpha$ -syn as site-specific Raman probes. (A) Structures of Met and HPG. HPG is readily incorporated into  $\alpha$ -syn by Met-auxotrophic *E. coli*. Schematic of  $\alpha$ -syn sequence showing acidic (red) and basic (blue) residues, as well as the fibrillar core determined by cryo-EM and the locations of Met residues replaced with HPG (asterisks). The C-terminal truncation site (115) is also indicated. (B) In the Raman spectrum, the alkyne stretching mode ( $C\equiv C$ ) of HPG- $\alpha$ -syn (purple) appears in the quiet region of the cellular background (black). (C) The alkyne

stretching band of HPG- $\alpha$ -syn<sub>1-115</sub> in cells (cyan) is narrower and blue-shifted relative to full-length HPG- $\alpha$ -syn<sub>1-140</sub> fibrils *in vitro* (purple) and in cells (magenta) as well as HPG- $\alpha$ -syn<sub>1-115</sub> *in vitro* (blue). The cell background (black) is shown for comparison. Data originally published in [27].

Author Manuscript

Author Manuscript

Author Manuscript

Author Manuscript